Zero degree polarization transfer measurements for the $^{13}C(\vec{p},\vec{n})^{13}N$ reaction at 197 MeV and empirical Gamow-Teller strength distribution

X. Wang, J. Rapaport, M. Palarczyk,* C. Hautala, and X. Yang
Ohio University, Athens, Ohio 45701

D. L. Prout†
Department of Physics, Kent State University, Kent, Ohio 44242

I. Van Heerden‡
Indiana University Cyclotron Facility, Bloomington, Indiana 47405

R. Howes and S. Parks
Ball State University, Muncie, Indiana 47306

E. Sugarbaker
The Ohio State University, Columbus, Ohio 43210

B. A. Brown
Michigan State University, East Lansing, Michigan 48824
(Received 18 September 2000; published 22 January 2001)

In this paper, we present differential cross sections and complete sets of polarization transfer coefficients, D_{ij}, obtained in the $^{13}C(\vec{p},\vec{n})^{13}N$ reaction studied at zero degree and at 197 MeV incident proton energy. The complete set of polarization observables is used to obtain the Fermi and Gamow-Teller (GT) cross section contributions in the ground state transition, which are then used to deduce GT transition strengths. The sum of the GT strength up to 20 MeV of excitation is compared with shell model calculations. In the region between 20 to 46 MeV of excitation, the differential cross section has been separated in spin and nonspin components.

DOI: 10.1103/PhysRevC.63.024608 PACS number(s): 25.40.Kv, 24.10.Eq

I. INTRODUCTION

Experimental studies of the (p,n) reaction at intermediate energies have provided extensive information on isovector modes of excitation in nuclei. Specifically, empirical proportionality factors have been used to relate $0°$ (p,n) differential cross sections to the Fermi (F) and Gamow-Teller (GT) strengths for the corresponding transitions [1]. Subsequently, studies of nuclides throughout the Periodic Table have established that the Gamow-Teller strength $B(\mathrm{GT})$, integrated up to about 20 MeV excitation energy, is only a fraction of the strength estimated in the same energy region from nuclear structure calculations for light and medium mass nuclei or from the sum rule limit for heavy nuclei [2,3]. More recently Wakasa *et al.* [4] have studied the Gamow-Teller strength of ^{90}Nb in the continuum via multipole decomposition analysis of the $^{90}Zr(p,n)^{90}Nb$ reaction at 295 MeV. The $B(\mathrm{GT})$ strength integrated up to 50 MeV yields a value $(93\pm5)\%$ of the minimum value of the sum rule.

A direct method of probing the spin-transfer character of a given transition is measuring polarization transfer observables. These observables are, in general, less sensitive to distortion effects than are differential cross sections or analyzing powers. They are easier to interpret and extremely useful in studies of the location of Gamow-Teller strength [5]. Such measurements have been performed at the Indiana University Cyclotron Facility (IUCF) with energies up to 200 MeV, at the Los Alamos National Laboratory Neutron Time Of Flight (NTOF) facility [6], with energies up to 800 MeV and at the Research Center for Nuclear Physics in Osaka, Japan with energies up to 400 MeV [7].

Mirror-state transitions between $T=\frac{1}{2}$ nuclei have been a favored testing ground for Gamow-Teller studies because parent and daughter states differ only in isospin projection. The transition rate between mirror states is the incoherent sum for the Fermi and Gamow-Teller components. All the Fermi strength $B(F)=1$ and a fraction of the GT strength appears in the mirror state transition, while the remaining part of the GT strength is located in excited states. In general only a small fraction of the total GT strength is contained in the mirror-state transition. Measurements of GT strength distribution in C isotopes using the $(\vec{p},\vec{n})$ and/or the (p,n) reaction have been reported by Goodman [8] and Rapaport [9]. In this paper we present differential cross section and a complete set of polarization transfer coefficients for the $^{13}C(\vec{p},\vec{n})^{13}N$ reaction at $0°$ obtained using the INPOL [10]

*Permanent address: Henryk Niewodniczański Institute of Nuclear Physics, 31-342 Kraków, Poland.
†Permanent address: U.S. DOE Remote Sensing Laboratory, Las Vegas, NV 89115.
‡Permanent address: University of the Western Cape, South Africa.

facility at IUCF. The data were obtained with 197 MeV protons, and we present results up to 46 MeV of excitation in ^{13}N. The complete set of $(\vec{p},\vec{n})$ polarization transfer coefficients for the ground state (g.s.) transition, is used to obtain the fraction of the GT contribution to the zero degree differential cross section.

II. EXPERIMENTAL METHOD AND DATA ANALYSIS

The experiment was performed using the Indiana Neutron POLarization (INPOL) facility at IUCF. Polarized protons with an energy of 197 MeV were focused on a self-supported $(89\pm4)\%$ isotopically enriched ^{13}C target with a total thickness of 146 mg/cm^2. The enrichment of the target was measured with an inductively coupled plasma mass spectrometer. For completeness, a short description of INPOL is presented, while more details may be found in Ref. [10].

The high intensity polarized ion source (HIPIOS) [11] was used to provide 70% polarized proton beams with intensities up to 380 nA in subnanosecond pulses separated by about 170 ns. The beam polarization was cycled between ''normal'' and ''reverse'' at 30 s intervals. Superconducting solenoids located in the proton beam line were used to precess the proton spin polarization so as to have on target either of the three spin states, normal $(\hat{N})$, sideways $(\hat{S})$, and longitudinal $(\hat{L})$. The settings on the solenoids take into account the precession caused by the swinger magnets. Values of the proton beam polarization were continuously measured with beamline polarimeters located immediately after the superconducting solenoids [12].

Dipole magnets, located after the target were used to precess the longitudinal neutron spin into a direction normal to its momentum in order to make the longitudinal component measurable in the neutron polarimeters. To correct for possible geometrical polarimeter asymmetries, superconducting solenoids located after the target were used to flip the neutron spin direction.

A large volume neutron polarimeter located in the 0° neutron beam line was used to measure the polarization of neutrons emitted in the ^{13}C$(\vec{p},\vec{n})^{13}$N reaction. The polarimeter consists of four parallel detector ''planes'' oriented perpendicular to the incident neutron flux. Each 1 m^2 ''plane'' consists of ten scintillators each 10-cm high, 10-cm thick, and 1-m long. The front two scintillator planes are used as neutron polarization analyzers. Time, position, and pulse-height information from front and back planes are used to kinematically select $n+p$ interactions, and to provide the analyzing power to measure the neutron polarization. Thin plastic scintillators in front of these planes are used to tag charged particles. Intrinsic time resolution of about 300 ps full width at half maximum (FWHM) and position resolution of about 4.5 cm (FWHM) are usually obtained. The neutron flight path to the first plane of these detectors was measured to be 159 m.

Neutron energies were measured by time-of-flight from the target to the front detector with an overall energy resolution that depends on target thickness and that was about 600 keV (FWHM) for the studies of ^{13}C at 197 MeV incident proton energy. In a separate experiment at 160 MeV incident proton energy and at 0° on a thinner ^{13}C target (50 mg/cm^2), the neutron energy resolution was about 200 keV. This additional study was done to attempt to resolve weak and close lying transitions in ^{13}N.

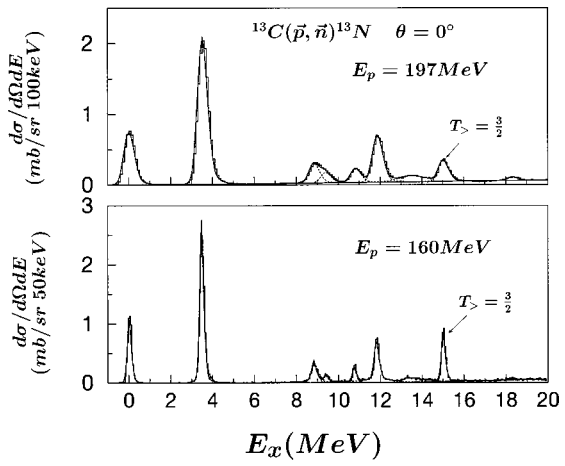

FIG. 1. Zero degree excitation energy spectra for the ^{13}C$(p,n)^{13}$N reaction obtained at $T_p=197$ MeV (top) and at $T_p=160$ MeV (bottom). The solid line represents the sum fitting to the data. Individual peak-fits are shown as dotted lines. (See text, Sec. II.)

Absolute differential cross sections were obtained using the method described in Ref. [10]. Briefly, the product of the neutron detector efficiency for double scattering and the neutron absorption in air and other material over the 159 m neutron flight path, was measured empirically using the ^{7}Li$(\vec{p},\vec{n})^7$Be reaction under similar experimental conditions. The 0° differential cross section for this reaction is well known from activation measurements in the energy range between 80–800 MeV [13]. The neutron energy dependence for these normalization factors has been obtained previously [10]. Uncertainties in the measured cross sections listed in the tables are only statistical. To obtain absolute uncertainties one needs to add in quadrature a 7% error due to uncertainties in target thickness, enrichment of ^{13}C and neutron polarimeter efficiency.

In Fig. 1, we present 0° spectra obtained at proton incident energies of 197 MeV (top spectra) and at 160 MeV (bottom spectra). The latter spectra was obtained in a previous different experiment. The better energy resolution obtained at the lower incident energy permitted a clear separation of the excited states in ^{13}N at 8.92 and 9.48 MeV [14] which were not resolved at the higher energy.

Fitting of the spectra was performed with the line-shape fitting code ALLFIT [15], a versatile fitting program suitable to analyze spectra in a large variety of nuclear reactions for a large range of excitation energy. The search code employs a Poisson rather than a Gaussian goodness-of-fit criterion. The fitting function was chosen to be composed of a background $B(x)$ and a sum of individual peaks $y_i(x)$, such that

$$y(x)=B(x)+\sum_{i=1}^{n} y_i(x), \tag{1}$$

TABLE I. Experimental differential cross sections and polarization transfer coefficients D_{ij} for the $^{13}C(\vec{p},\vec{n})^{13}N$ reaction at $T_p=197$ MeV and $\theta_{lab}=0°$. All errors indicated as superscripts are statistical only. The excitation energy values are from Ref. [13] except for the state with a superscript ''a,'' which is characterized in this work as a GT transition. The excitation energy values with a superscript ''b'' correspond to states with $T=3/2$.

E_x(MeV)(J^π)	$\sigma_{c.m.}(0°)$ (mb/sr)	D_{NN}	D_{SS}	D_{LL}	sum D_{ij}
0.00 $((1/2)^-)$	3.90^{2}	-0.06^{3}	-0.008^{20}	-0.08^{2}	-0.15^{4}
3.50 $((3/2)^-)$	10.77^{4}	-0.32^{2}	-0.33^{2}	-0.36^{2}	-1.01^{3}
8.92 $((1/2)^-)$	1.49^{2}	-0.19^{7}	-0.40^{5}	-0.41^{5}	-1.00^{10}
9.48 $((3/2)^-)$	0.77^{2}	-0.49^{12}	-0.29^{8}	-0.29^{9}	-1.07^{17}
10.83$((1/2)^-)$	1.07^{1}	-0.34^{7}	-0.32^{5}	-0.48^{5}	-1.14^{10}
11.74 $((3/2)^-)$	3.51^{3}	-0.35^{4}	-0.27^{2}	-0.47^{3}	-1.09^{6}
13.5^{a} $((1/2)^-;(3/2)^-)$	1.08^{5}	-0.24^{19}	-0.24^{12}	-0.35^{18}	-0.83^{29}
15.06^{b} $((3/2)^-)$	1.60^{3}	-0.25^{5}	-0.20^{4}	-0.41^{6}	-0.86^{9}
18.17 $((1/2)^-)$	0.27^{1}	-0.32^{23}	-0.23^{17}	-0.66^{27}	-1.22^{39}
18.96^{b} $((3/2)^-)$	0.08^{1}				

where x is the laboratory neutron energy. The background function is a polynomial of up to third order and can contain continuous segments for targets with a decay threshold. Each peak can be described as the convolution

$$y_i(x)=I_i(x)\otimes R_i(x) \tag{2}$$

of an intrinsic line shape $I(x)$ with a resolution function $R(x)$ which represents the effects of neutron spectrometer resolution, target thickness, and beam properties. The standard resolution function consists of an asymmetric hyper-Gaussian in the central region plus exponential tails [16]. States with negligible intrinsic width were described by the resolution function alone. States with non-negligible width were described by Lorentzian line shapes convoluted with the resolution function.

The fitting procedure was started by fitting the ground state transition, which corresponds to a well isolated peak to obtain the best parameters for the corresponding line shape. Then the spectrum obtained at 160 MeV was fitted up to 20 MeV excitation energy by locking positions of known excited states in ^{13}N [14] with quantum numbers corresponding to GT transitions. Including the g.s. transition, a total of nine excited states are listed in ^{13}N that meet that criterion [14]. The natural widths for the 8.92 and 11.74 MeV states are 230 and 530 ± 80 keV, respectively. These widths were added in quadrature to the experimental resolution (190 keV) to properly fit the shape of these peaks. One additional small peak at 13.5 MeV with a different line shape corresponding to a larger width was needed to obtain an overall lower χ^2 for the entire fitted energy region. Although there is a state at 13.5 ± 0.2 MeV with a natural width of 6500 keV reported in Ref. [14], it is reported with a $J^\pi=(3/2)^+$ that corresponds to a dipole ($\Delta L=1$) transition. We believe that the state excited in the (p,n) reaction is not the one listed in the above reference. A preliminary analysis of (p,n) data taken at other angles, 6° and 9°, indicates that the observed transition has an $L=0$ character, and we assign it here as a GT transition based on its angular distribution shape and D_{ij} values (see Table I). The same set of excited states were used in the fitting of the 197 MeV data, also up to 20 MeV excitation energy, both for the differential cross section analysis and for the polarization transfer analysis. Typical $\chi^2\approx6.7$ per degree of freedom were obtained. Figure 1 shows representative fitted spectra obtained at 160 and 197 MeV.

A. EXPERIMENTAL RESULTS

The method outlined in the previous section has been used to fit all the states observed in the 0° $^{13}C(\vec{p},\vec{n})^{13}N$ spectra up to an excitation energy of 20 MeV. Beyond that excitation energy, only a smooth continuum cross section characterizes the spectrum. We present the spectrum up to 46 MeV of excitation in Fig. 2. In the region between 20 and 46 MeV of excitation, a correction had to be applied to the data to account for a small fraction (approximately 5%) of the proton beam energy delivered on target about 60 ns later than the primary beam. The IUCF cyclotron operates at a frequency close to 35 MHz, which yields a proton pulse separation of about 29 ns. For the (p,n) time-of-flight experiments, we ran INPOL selecting one-in-six beam pulses, to provide proton pulses separated by about 170 ns. However, the pulse selection is imperfect and satellite peaks sometimes appear from the proton bursts that are not completely rejected. In this case a superimposed satellite spectrum appears on the main neutron time-of-flight spectrum at a high excitation energy region. The satellite spectrum was subtracted and the beam current integrator was corrected to account for the fraction of the proton beam not in the main pulse. The results are displayed in Fig. 2. Because of the continuum character of the 0° differential cross section above 20 MeV of excitation, we decided to sum the yields in energy bins of 2.5 MeV and to obtain the differential cross section as well as the D_{ij} coefficients in that manner.

As indicated earlier, the enrichment of ^{13}C in the target was $(89\pm4)\%$. Thus the target contained 11% of ^{12}C. Spectra obtained with a ^{nat}C target, 99% ^{12}C, were properly subtracted and the results are shown both in Figs. 1 and 2. The

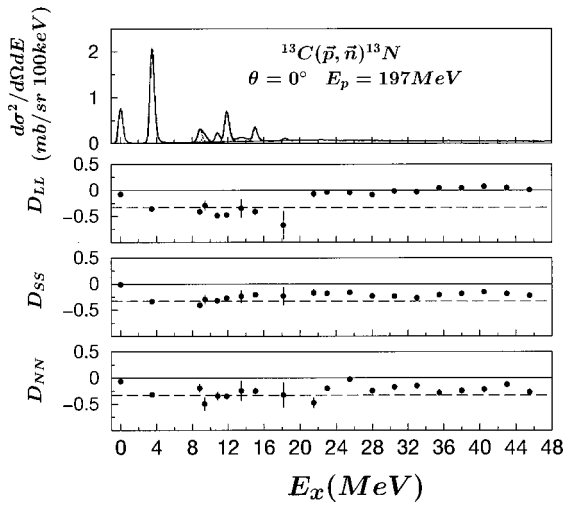

FIG. 2. Zero degree excitation energy spectra for the $^{13}C(p,n)^{13}N$ reaction obtained at $T_p=197$ MeV is shown in the top frame. The other three frames represent D_{ij} coefficients. In these frames, the dash line corresponds to the canonical value $D_{ij}=-1/3$ for GT transitions. Data up to 20 MeV excitation correspond to values obtained by fitting individual peaks shown in the top frame while data above 20 MeV represent integrated values in 2.5 MeV bins.

main contribution of the ^{12}C is due to its g.s. which has the same Q-value as the $^{13}C(p,n)^{13}N$ transition to the 15.1 MeV excited state.

The top of Fig. 2 shows the differential cross section while the other three sections of the figure show values for D_{LL}, D_{SS}, and D_{NN}, respectively. Up to 20 MeV of excitation the values for D_{ij} obtained from the fitted spectra are presented, while results in energy bins of 2.5 MeV are shown in the region between 20 and 45 MeV of excitation. The $D_{NN}(0^\circ)$ values should be equal to the $D_{SS}(0^\circ)$ values since both transverse directions are identical. The experimental $D_{NN}(0^\circ)$ values are consistent with the corresponding $D_{SS}(0^\circ)$ values, pointing the high reliability of the present measurements. The D_{LL} values, which are negative up to about 20 MeV of excitation, become close to zero at higher excitation energies and in some regions small but positive. The energy region up to 20 MeV is characterized by similar values approximately -0.33, of all the D_{ij} coefficients, while above 20 MeV of excitation the transverse coefficients are close to -0.2 and the spin longitudinal coefficients close to 0.0. The sum of the D_{ij} coefficients for all the observed transitions up to about 20 MeV of excitation is close to -1.0, in agreement with these transitions being GT transitions.

III. EXTRACTION OF THE GT STRENGTH

In their study of the (p,n) reactions on the mirror nuclei ^{13}C and ^{15}N, Goodman *et al.* [8] have pointed out that the major $(1/2)^- \rightarrow (3/2)^-$ transitions are strongly quenched relative to the $(1/2)^- \rightarrow (1/2)^-$ mirror transitions. This result strongly disagrees with simple shell model expectations. The g.s. mirror transitions are an incoherent sum of the rates for the Fermi and Gamow-Teller components. Since all the Fermi strength is contained in the mirror transition, the measured β-decay ft value is used to obtain the empirical GT strength. The g.s. cross section in mb/sr is decomposed into its Fermi and GT contributions. These values are then divided by the corresponding Fermi and β-decay GT strength to obtain the Fermi and GT unit cross sections, $\hat{\sigma}_{\rm F}$ and $\hat{\sigma}_{\rm GT}$, respectively.

Goodman *et al.* [8] have used the empirical $\hat{\sigma}_{\rm GT}$ to normalize the (p,n) cross section in GT units. Measurements of the spin-flip probability S_{NN} are used to give an independent determination of the GT fraction in the g.s. cross sections.

Comparison of the g.s. GT strength to a shell model transition strength results in a quenching of 0.66, which is consistent with the quenching observed in other nuclei [2]. However, the calculated B(GT) value of the strongest transition, that to the 3.50 MeV excited state, is nearly a factor of 3 larger than the value deduced from the (p,n) measurements. This issue has also been studied by Watson *et al.*, [17], and they point out that for odd-nuclei targets the renormalization of the GT operator needed for (p,n) reactions is different from that needed for β-decay. These authors introduce an effective (p,n) GT operator that includes matrix elements with coefficients empirically obtained from a least-squares fit to known transitions in nuclei with $A \leqslant 18$ [18]. The calculations indicate that the mirror g.s. transition appears 1.87 larger in (p,n) than if it were exactly proportional to the β decay GT value. They therefore question the conclusions reached by Goodman *et al.* We revisit this problem in the next paragraphs.

The normalization of the 0° (p,n) differential cross section in GT units is a delicate issue for $^{13}C(p,n)^{13}N$ reaction. If we follow the procedure indicated by Goodman *et al.* [8], the present results agree well with those reported in that reference. However, the effective (p,n) GT operator suggested in Ref. [17], includes coherent terms which do not appear in the β-decay GT calculation. Thus, such a normalization would be erroneous.

There are several possible alternatives to obtain the GT unit cross section which will be discussed in detail later. One possibility would be to compare the empirical (p,n) cross section to the shell model calculated value for the strong GT transition at 3.5 MeV. The advantage of this method is that the calculated value is rather insensitive to theoretical assumptions with respect to the operator used (see below and Table II). However, this comparison would not be in the spirit of previous studies that have relied mainly on empirical results. Another approach is to use the transition to the $T_>=3/2$ excited state in $^{13}N(15.1\ {\rm MeV})$ for which the β-decay GT strength may be inferred from the β-decay of ^{13}B. A third possibility is to obtain the Fermi and GT contributions to the mirror g.s. transition, and normalize the Fermi to its $B({\rm F})=1$ strength value. Then, use the empirical ratio between $\hat{\sigma}_{\rm GT}$ and $\hat{\sigma}_{\rm F}$ obtained for even nuclei by Taddeucci *et al.* [1] to obtain $\hat{\sigma}_{\rm GT}$.

In the next few paragraphs we present the results of some of these normalizations, but first we discuss the empirical method used to obtain the Fermi and GT contributions to the 0° g.s. mirror transition cross section.

TABLE II. Shell model calculations for B(GT) and $B(p,n)$ values for the ^{13}C$(p,n)^{13}$N reaction. The calculations assume 0 $\hbar\omega$ $1p$ transitions, and we used the WBT interaction with the OXBASH code.

E_x(MeV)(J^π)	B(GT) free	B(GT) eff	B(p,n) eff
0.00 $((1/2)^-)$	0.228	0.1746	0.3265
3.77 $((3/2)^-)$	2.068	1.3444	1.2530
8.795 $((1/2)^-)$	0.4631	0.2976	0.2525
10.85 $((3/2)^-)$	0.4712	0.3003	0.2666
13.17 $((3/2)^-)$	0.2279	0.1509	0.1438
13.645 $((3/2)^-)$	0.4355	0.2854	0.2934
14.387[a] $((3/2)^-)$	0.4434	0.2849	0.2545
17.235 $((3/2)^-)$	0.002	0.0018	0.0023
17.701 $((1/2)^-)$	0.0000	0.0002	0.0015
18.084 $((3/2)^-)$	0.0019	0.0012	0.0011
19.191[a] $((1/2)^-)$	0.0054	0.0042	0.0091
22.802[a] $((3/2)^-)$	0.0002	0.0001	0.0000
24.050 $((1/2)^-)$	0.0009	0.0006	0.0006
27.552[a] $((3/2)^-)$	0.0004	0.0003	0.0002
Sum	4.348	2.846	2.805

A. F and GT contributions to the g.s. mirror-state transition

The complete set of $(\vec{p},\vec{n})$ polarization transfer coefficients reported here for the first time on a ^{13}C target, gives us a unique method to obtain the Fermi (nonspin) and Gamow-Teller (spin) components in the g.s. mirror-state transition. Using Eq. (7) (See Sec. III F) and the D_{ij} values from Table I, we get that the fraction of nonspin cross section in the mirror g.s. transition is $21\pm1\%$. Thus the GT fraction in the ground state transition is $79\pm1\%$.

Values for this fraction have been obtained by other authors at incident proton energies between 50 and 200 MeV. Sakai *et al.* [7] have reported data at 50 and 80 MeV. Taddeucci *et al.* [1] have reported data at 120, 160, and 200 MeV, and Watson and Du, [19] at 135 MeV. All the data are presented in Fig. 3, where the solid line has been obtained with the expression [8]

$$f_{\rm GT}=[1+B({\rm F})/B_M({\rm GT})R^2]^{-1}, \tag{3}$$

where $R=E_p/E_o$ with a fit value $E_{o,M}=(47\pm3)$ MeV, and M refers to the mirror g.s. transition. The $E_{o,M}$ value is different from $E_o=55\pm0.4$ MeV reported by Taddeucci *et al.* [1] as determined from the ^{14}C$(p,n)^{14}$N reaction at incident energies between 50 and 200 MeV. We believe that the discrepancy is due to the nonproportionality between the β-decay B(GT) and the corresponding 0° (p,n) cross section for the ^{13}C$(\vec{p},\vec{n})^{13}$N(g.s.) reaction.

B. THEORETICAL EVALUATIONS OF THE B(GT)

The mirror g.s. transition for the ^{13}C$(p,n)^{13}$N reaction contains a significant component of the $p_{1/2}\rightarrow p_{1/2}$ particle-hole transition. This is sometimes called a ''jackknife'' transition where the change in angular momentum and the change in spin have opposite phases, $j_i=l-1/2\rightarrow j_f=l-1/2$.

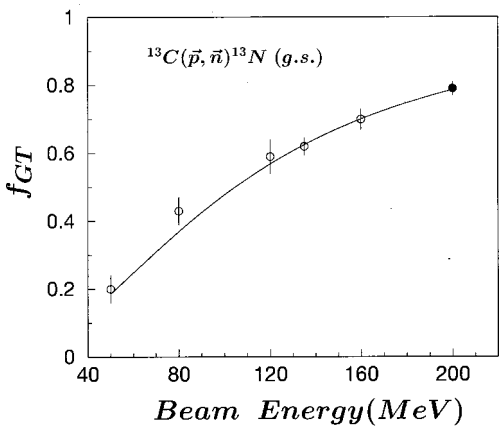

FIG. 3. Fraction of Gamow-Teller differential cross section for the ^{13}C$(p,n)^{13}$N(g.s.) at 0° versus proton beam energy, E_p. See text for equation used to represent the solid curve. The data point indicated with a solid circle is from the present work. See text for other references.

We have performed calculations to obtain B(GT) values for transitions in the ^{13}C$(p,n)^{13}$N reaction. The shell-model code OXBASH [20] was used to calculate the one body density matrix elements (OBDME). Only $0\hbar\omega$ $p\rightarrow p$ transitions are included. The OBDME values were obtained using the interaction derived by Warburton and Brown (WBT) which was obtained by a least-square fits to 51 $1p$-shell and 165 cross-shell binding energies [21]. The following types of B(GT) calculations were performed:

(a) Using an operator representing the free-nucleon B(GT).

(b) Using an effective B(GT) operator which is essentially the same as (a), but using an empirical quenching obtained from a comparison between calculations using (a) and experimental β-decay results for Gamow-Teller matrix elements for $A\leqslant18$ decays [18].

(c) Using an effective (p,n) operator. This operator includes effects of the nuclear medium and has been expressed via deviations from the free-nucleon values with empirical coefficients δ_s, δ_l, and δ_p. For free nucleons $\delta_s=0$. In calculations for GT β decay when one uses δ_s, δ_l, and δ_p, δ_s is most important and δ_l and δ_p are small. However, for (p,n) transitions δ_p has an empirically enhanced value compared to the β-decay operator [17]. The δ_p coefficient is particularly important for the ''jackknife'' transition which enters into the g.s. mirror transition. Thus, these calculations for matrix elements involved in the (p,n) reaction should *not* be confused *nor* labeled B(GT) values which are intrinsic to GT operators. The empirical values for the δ_s, δ_l, and δ_p coefficients for β-decay are taken from Ref. [21] and the enhanced value of δ_p for (p,n) reactions is taken from Ref. [17].

The results of these calculations are indicated in Table II. The sum B(GT) is about the same for the last two columns and is about 65% of the value predicted with the free nucleon

GT operator shown in the first column. However, values for specific transitions are not the same, particularly for the g.s. transition. On the other hand, the strong transition to the 3.5 MeV state, mainly a $(1/2)^-$ to a $(3/2)^-$ transition, has similar strength in the β decay and in the (p,n) calculations. This comparison between the shell model calculated values indicates that there is something special about the mirror transition and that using the g.s. β-decay B(GT) to normalize GT strength in (p,n) reactions may not be correct.

C. Distorted wave calculations

Differential cross sections and D_{ij} coefficients were theoretically obtained with microscopic distorted-wave impulse approximation (DWIA) calculations. These were done using the computer code DW81 [22] in which the knock-out exchange amplitudes are treated exactly. The three basic ingredients needed in this code, are briefly outlined below.

The free nucleon-nucleon interaction parametrized by Franey and Love [23] was used as the interaction between the incident and struck nucleons. The set of interaction parameters reported at $E_p = 210$ MeV were used in the DWIA calculations. A more recent parametrization developed by Love [24] produced almost identical results.

The OBDME, obtained as described in the previous section, were used for the nuclear structure part. Harmonic oscillator (HO) wave functions were assumed for the single particle states. In DWIA calculations for light nuclei, the center of mass corrections are important. These corrections were made as described by Brady *et al.* in the Appendix of Ref. [25]. A reduced HO size parameter $b_o = 1.87$ fm was used to calculate single particle states. This reduced HO size parameter is based on the analysis of the transverse form factor obtained from the (e,e') scattering on ^{13}C [26].

Distorted waves for incident an outgoing nucleons were calculated using optical model potential (OMP) parameters obtained from proton elastic scattering data for ^{12}C [27]. The energy dependence of OMP parameters was taken into account as suggested in Ref. [27]. The isospin effect as well as the Coulomb correction potential were applied to the OMP parameters for describing the unpaired nucleon [28].

Using the procedure described in Ref. [1], we have calculated the function F(q,ω) where q is the momentum transfer and ω is the energy loss. This was done for each excited state calculated from the shell model with the corresponding OXBASH OBDME. The curve representing the set of values as a function of energy loss ω is shown in Fig. 4. This function is used to extrapolate the measured 0° differential cross section at a particular q and ω to that value at $q = \omega = 0$ in order to normalize the differential cross section in units of GT strength. It is clear from the figure that a correction of almost a factor of 2 at an excitation energy of about 30 MeV would be needed. This large correction and its intrinsic uncertainty estimated to be at least 10–15% due to uncertainties in OMP parameters and other parameters needed in the calculations, renders questionable the use of this procedure at high excitation energies.

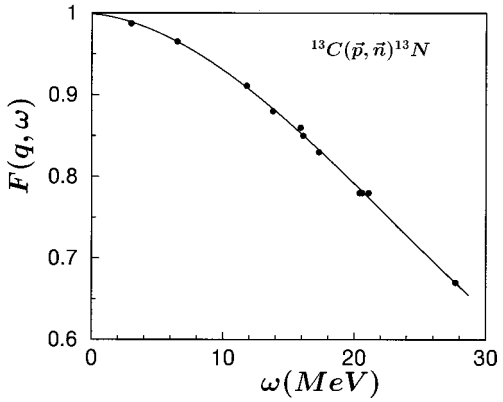

FIG. 4. Correction function F(q,ω) obtained using DWIA calculations for the shell model excited states in ^{13}N.

D. The unit GT cross section and B(GT) values

The measured $\sigma(q,\omega)$, $\Delta L = 0$, $\Delta S = 1$, zero degree (p,n) differential cross sections may be written in a factorized expression [1]:

$$\sigma(q,\omega) = F(q,\omega) * \hat{\sigma}_{\mathrm{GT}}(E_p,A) * B(\mathrm{GT}), \tag{4}$$

where F(q,ω) is the calculated function used to extrapolate the cross section to its value at $(q=0,\omega=0)$, and which goes to unity in the limit of zero momentum transfer and energy loss. The symbol $\hat{\sigma}_{\mathrm{GT}}$ represents the unit GT cross section. To normalize the measured (p,n) zero degree differential cross section in GT units, the value for $\hat{\sigma}_{\mathrm{GT}}(A,E_p)$ which depends on atomic mass number A, and incident energy E_p, must be known. It may be calculated if the corresponding B(GT) strength for that transition is empirically known from its β-decay ft value. In the present case, the mirror transition which is a mixed Fermi and Gamow-Teller transition, has a β-decay $B(\mathrm{GT}) = 0.202 \pm 0.016$ [14]. The present spin transfer measurements indicate that $f_{\mathrm{GT}} = 0.79 \pm 0.01$ is the fraction of GT cross section in the mirror transition, i.e., it has a cross section of 3.08 ± 0.04 mb/sr. Thus, we obtain $\hat{\sigma}_{\mathrm{GT}} = 15.2 \pm 0.8$ mb/sr and $\hat{\sigma}_{\mathrm{F}} = 0.82 \pm 0.04$ mb/sr for the GT and F unit cross sections respectively. The unit GT value may then be used to calculate the corresponding GT strengths for other GT transitions. Following this procedure, the present GT results are similar to those presented in Ref. [8]. However, as indicated in the previous paragraph, this normalization method may not be correct for the ^{13}C$(p,n)^{13}$N reaction.

The cross section could also be normalized to the strongest GT transition calculated from the shell-model, in this case the transition to the 3.50 MeV excited state. Using the average value from the last two columns in Table II, we get $\hat{\sigma}_{\mathrm{GT}} = 8.6 \pm 0.4$ mb/sr. However, this result is model dependent and is not truly an empirical result.

Another approach would be to use the transition to the $T_> = 3/2$ state at 15.1 MeV excitation in ^{13}N. A GT strength for that transition may be inferred from the β decay of ^{13}B. However, there is some difficulty involved in getting the

correct B(GT) which is associated with the well known rate asymmetry for mirror decays in the $A=12$ and $A=13$ systems [29]. Taddeucci *et al.* [1] estimate a value $B(\mathrm{GT})=0.23\pm0.01$ for the transition $^{13}\mathrm{C}(p,n)^{13}\mathrm{N}(15.1\ \mathrm{MeV})$ where the uncertainty assigned to this value comes from the rate asymmetry. The spectrum shown in Fig. 1 clearly indicates the excitation for that transition. However, the $^{12}\mathrm{C}(p,n)^{12}\mathrm{N}$(g.s.) transition has the same Q value as the $^{13}\mathrm{C}(p,n)^{13}\mathrm{N}(15.1\ \mathrm{MeV})$ transition, and it has a differential cross section about four times larger. Thus, a small admixture of ^{12}C in the ^{13}C target makes a large uncertainty in the $^{13}\mathrm{C}(p,n)^{13}\mathrm{N}(15.1\ \mathrm{MeV})$ differential cross section. Mildenberger *et al.*, [30] report a value $\hat{\sigma}_{\mathrm{GT}}=9.8\pm0.8$ mb/sr for the $^{13}\mathrm{C}(p,n)^{13}\mathrm{N}(15.1\ \mathrm{MeV})$ transition also studied at 200 MeV incident energy. This value is consistent with the present result, $\hat{\sigma}_{\mathrm{GT}}=8.5\pm1.0$ mb/sr. In the present study a larger uncertainty is assigned to the cross section for this transition, because of the uncertainty in the admixture of ^{12}C in the target.

Alternatively an empirical approach can be employed in cases where there is no known β-decay information for the transitions measured in the (p,n) reaction. This approach consists of normalizing to the Fermi transition and using the empirical ratio between unit GT and unit F cross sections obtained with even targets in the (p,n) reaction [1]. This ratio is the square of (E_p/E_o) where $E_o=55.0\pm0.4$ MeV. Using $\hat{\sigma}_{\mathrm{F}}=0.82\pm0.04$ mb/sr for the g.s. mirror transition, we deduce $\hat{\sigma}_{\mathrm{GT}}=10.5\pm0.5$ mb/sr.

The last three results for $\hat{\sigma}_{\mathrm{GT}}$ (8.6 ± 0.4, 8.5 ± 1.0, and 10.5 ± 0.5 mb/sr) are not too different from each other, but quite different from the first value, $\hat{\sigma}_{\mathrm{GT}}=15.2\pm0.8$ mb/sr. We choose to use $\hat{\sigma}_{\mathrm{GT}}=10.5\pm0.5$ mb/sr to report B(GT) values for the GT transitions studied in this paper. This value does not rely on an absolute shell-model calculation, agrees with the value for the $T_>$ transition to the 15.1 MeV excited state in ^{13}N, and, as mentioned above, it has been obtained with the method used in cases where the (p,n) reaction does not excite states with known β-decay information but where there is information for the IAS transition. This new value $\hat{\sigma}_{\mathrm{GT}}=10.5\pm0.5$ mb/sr also indicates a smooth atomic number A dependence of $\hat{\sigma}_{\mathrm{GT}}$. See Ref. [1].

We report B(GT) values for excited states observed in this study in Table III. The measured cross sections extrapolated to $q=\omega=0$ are indicated in the first column. These are the center of mass cross section values from Table I divided by $\mathrm{F}(q,\omega)$. The GT value for the g.s. transition is that from β-decay. The sum B(GT) for these states is about 54% of the value calculated using the free-nucleon β-decay interaction in the shell model.

E. Additional GT strength

The question of the ''missing'' GT strength has received much experimental and theoretical attention over the past few years. Two physically different mechanisms have been proposed to explain this quenching of the total GT strength. In the first, the $\Delta(1232)$ isobar nucleon-hole states (ΔN^{-1}) couple into the proton-particle neutron-hole (pn^{-1}) GT states resulting in a part of the GT strength being moved from the low excitation region to the Δ excitation region at around 300 MeV excitation [31–33]. The second mechanism is nuclear configuration mixing, [34–36] in which energetically high lying two-particle, two-hole ($2p2h$) states mix with the low-lying $1p1h$ GT states, and shift GT strength into the energy region beyond the main peaks of the GT region. With this mechanism, the ''missing'' GT strength would actually be located in the physical background below and beyond the main GT region, in the present case above 20 MeV of excitation in ^{13}N. The ''missing'' GT strength question does not have an easy empirical answer because the $0°$ (p,n) differential cross section above 20 MeV of excitation is usually continuous and structureless. Bertsch and Hamamoto [35] have performed a perturbative calculation for the mixing of GT strength with $2p2h$ configurations at high excitation energies. They found that about 50% of the total GT strength could be shifted into the region of 10–45 MeV excitation energy for the nucleus ^{90}Zr. Using a multipole decomposition (MD) analysis and a complete set of polarization observable at $0°$, Wakasa *et al.* [4] have studied the $^{90}\mathrm{Zr}(\vec{p},\vec{n})^{90}\mathrm{Nb}$ reaction at 295 MeV. Their results indicate that approximately 90% of the Ikeda sum rule [37], $3(N-Z)=30$, has been located up to 50 MeV of excitation.

TABLE III. Zero degree differential cross section extrapolated to $q=\omega=0$ and empirical B(GT) values for the $^{13}C(p,n)^{13}$N reaction. Uncertainties in the c.m. cross sections are only statistical. An 8% uncertainty is estimated in the B(GT) values, mainly from the uncertainty in the unit GT cross section. The excitation energy with a superscript ''a'' corresponds to a $T=3/2$ state. The B(GT) for the g.s. transition denoted with a superscript ''b'' is the β-decay value.

E_x(MeV)(J^π)	$\sigma(q=\omega=0)$ (mb/sr)	B(GT)
0.00 ($(1/2)^-$)	4.00[2]	0.20[b]
3.50 ($(3/2)^-$)	11.16[4]	1.06
8.92 ($(1/2)^-$)	1.64[2]	0.16
9.48 ($(3/2)^-$)	0.86[2]	0.08
10.83 ($(3/2)^-$)	1.22[1]	0.12
11.74 ($(3/2)^-$)	4.08[3]	0.39
13.5 ($(1/2)^-$; $(3/2)^-$)	1.29[4]	0.12
15.06[a] ($(3/2)^-$)	1.95[4]	0.19
18.17 ($(3/2)^-$)	0.35[1]	0.03
Sum		2.35

In Fig. 2, we show the $0°$ double differential cross section and a complete set of polarization transfer observables D_{ij} as a function of excitation energy. The laboratory coordinates are defined so that the normal, $\hat{N}$, direction is normal to the scattering plane, the longitudinal, $\hat{L}$, direction is along the direction of momentum transfer and the sideways, $\hat{S}$, direction is given by $\hat{S}=\hat{N}\times\hat{L}$. The sum of the D_{ij} coefficients are presented in the middle part of Fig. 5, sum which for GT transitions should be equal to -1.0. This is in agreement with the observation that all fitted states up to 20 MeV of

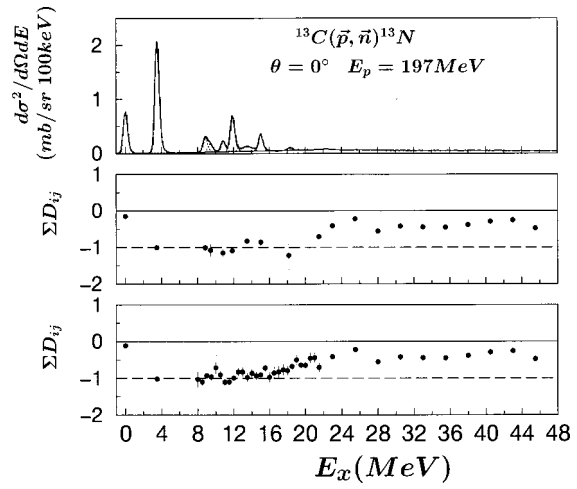

FIG. 5. Sum of all the D_{ij} coefficients as a function of excitation energy. The middle panel shows values obtained from individual peak fitting in the excitation energy region up to 18 MeV. The bottom panel presents values between 8 and 20 MeV of excitation obtained from data that have been binned in 0.5 MeV energy bins.

excitation, as shown in the top part of the figure, are GT transitions. Above 20 MeV of excitation, we have added the D_{ij} results from the spectra that have been sorted in 2.5 MeV bins. It is clear from the figure that, in this energy region, there are nonspin transfer transitions that contribute to the sum of the D_{ij} coefficients to be greater than -1.0. For pure nonspin transitions the sum should be $+3.0$.

In the excitation energy region between 8 and 18 MeV, a continuum background was needed to fit the spectra, as seen at the top of Fig. 5. In order to assess the character of such background, we have sorted the data into bins of 0.5 MeV and obtained the respective D_{ij} values. The sums of these D_{ij} coefficients are shown at the bottom of Fig. 5 and are all approximately equal to -1.0 indicating that in this region the excitations are predominantly spin transfer transitions. For excitation energies above about 18 MeV, the sum of the D_{ij} takes values between -0.3 to -0.4. Thus, if we assume that in the region underneath the resolved GT states (8 to 18 MeV) the excitations are just GT transitions, an additional $B(\mathrm{GT})=0.66$ units is obtained. Adding this GT strength to the one obtained for well resolved states, we obtain 3.01 GT units or about 69% of the value predicted by the shell model. It is very likely that more GT strength lies above 20 MeV of excitation. However, we do not have a reliable method to sort the possible $\Delta L=0$, $\Delta S=1$ components of the differential cross sections in this smooth energy region where other spin-flip resonances dominate. In addition, a large $\mathrm{F}(q,\omega)$ correction factor is needed to obtain the GT strength, which carries a large uncertainty. Charge exchange reaction data taken on the same target and at about the same energy [38] indicate that the dipole excitation in ^{13}N peaks around 22 MeV of excitation. For these reasons, we prefer to decompose the region between 20 and 50 MeV of excitation in terms of spin-flip and nonspin-flip cross sections. Nevertheless, an upper limit of GT strength in that region is estimated in next section.

F. Polarization observables

At 0° and within the plane wave impulse approximation (PWIA), there are simple relationships between the D_{ij}'s and the spin transfer character of the transition [39,40]. For spin flip transitions ($\Delta S=1$), the sum of the D_{ij} coefficients is equal to -1. Since the transverse coefficients are equal, $D_{NN}=D_{SS}=D_T$, we may write

$$2\times D_T(0^\circ)+D_{LL}(0^\circ)=-1. \tag{5}$$

Similarly for nonspin flip transitions, we have

$$2\times D_T(0^\circ)+D_{LL}(0^\circ)=3. \tag{6}$$

In the region of excitation between 18 and 46 MeV, some fraction of the excited states seems to have a nonspin flip character. This may be better visualized by decomposing the 0° double differential cross section into $\Delta S=1$ and $\Delta S=0$ partial cross sections. In addition, the $\Delta S=1$ differential cross section may be separated into spin-transverse and spin-longitudinal partial differential cross sections which pertain to the tensor character of the reaction [41]. These partial cross sections [42] at 0° are expressed simply as

$$I_o=\frac{1}{4}I_u(1+2D_T+D_{LL}), \tag{7}$$

$$I_q=\frac{1}{4}I_u(1-2D_T+D_{LL}), \tag{8}$$

$$I_p=I_n=\frac{1}{4}I_u(1-D_{LL}), \tag{9}$$

with the condition

$$I_u=I_o+I_q+I_p+I_n, \tag{10}$$

where I_o, I_q, I_p, and I_n correspond, respectively, to the spin independent, spin longitudinal, and the two spin transverse partial cross sections.

The middle panel of Fig. 6 displays the percentage of the zero degree double differential cross section characterized with spin transfer ($\Delta S=1$) in open circles, and the percentages of the spin independent ($\Delta S=0$) double differential cross section are presented in closed circles. Except for the mixed Fermi and GT g.s. transition, only in the excitation energy region above about 18 MeV, is there an appreciable (about 15%) percentage of spin independent excitation. The bottom panel of Fig. 6 presents the percentages of spin transverse and spin longitudinal double differential cross section with the condition that twice the spin transverse cross section plus the spin longitudinal cross section is equal to the spin dependent differential cross section. The data indicate that, within error bars, the longitudinal and either of the transverse double differential cross sections have equal magnitude throughout almost the entire excitation energy region analyzed in the present study.

The spin dependent zero degree double differential cross section above 20 MeV of excitation, may be used to obtain an upper limit of the GT strength in that energy region. We

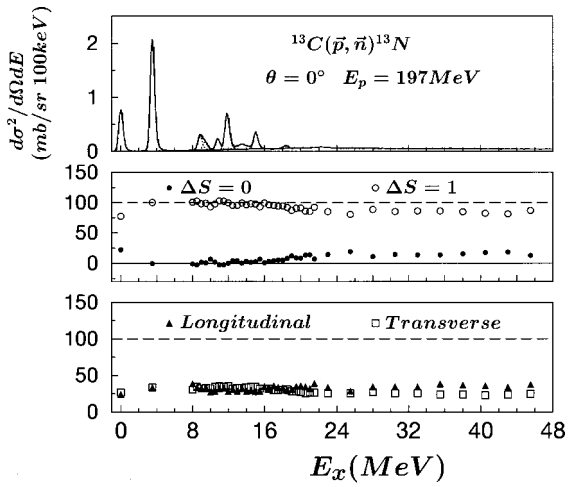

FIG. 6. Decomposition of the zero degree double differential cross section. In the middle panel open circles indicate the percentage of spin-flip cross section while the closed circles indicate the percentage of spin independent cross section. In the bottom panel the spin dependent double differential cross section has been decomposed in the percentage of spin longitudinal (closed triangles) and spin transverse (open squares) double differential cross section.

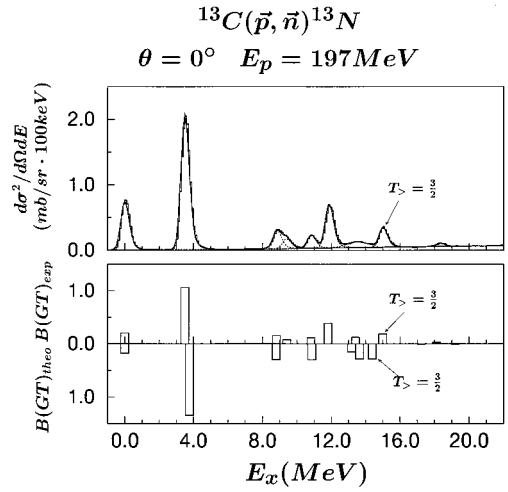

FIG. 7. Empirical GT strengths (Table III, third column) are compared to those from a shell model calculation (Table II, third column). The empirical g.s. $B(\mathrm{GT})$ corresponds to that from β-decay. All others are from this work.

will do that in the assumption that spin multipole resonances higher than $\Delta L=0$ are not excited at zero degree, which as explained above is not the case. We have calculated the energy integrated differential cross section in 2.5 MeV bins, extrapolated the cross section to $q=\omega=0$ and obtained the corresponding GT strength. Up to 48 MeV of excitation the sum GT strength amounts to an additional 2.4 GT units. However, part of the zero degree differential cross section in this energy region corresponds to multipoles higher than $L=0$, that will reduce the above sum GT strength value. To do a complete analysis for the GT strength in this region, it is also required to have empirical data from the $^{13}\mathrm{C}(n,p)^{13}\mathrm{B}$ reaction, which undoubtedly would show spin dependent cross section in this excitation energy region.

IV. CONCLUSIONS

We have presented double differential cross sections and spin transfer coefficients for the $^{13}\mathrm{C}(\vec{p},\vec{n})^{13}\mathrm{N}$ reaction obtained at $0°$ with $E_p=197$ MeV. The data are used to obtain GT strength for all the observed transitions as well as to estimate GT strength in the ''background'' region up to about 20 MeV. Comparing the results to a shell model calculation we estimate that we have obtained about 69% of the total shell model estimated GT strength. Above 20 MeV of excitation, contributions of spin independent differential cross section as well as longitudinal and transverse spin transfer have been obtained. In Fig. 7, we compare the GT strength observed in individual peaks to that of a shell model calculation with an effective operator that quenches the free GT strength to 60%. The shell model calculations were done using only $0\hbar\omega$ particle-hole excitations, and thus, as expected, the calculations concentrate the strength to low lying states. It is very likely that a calculation using more extensive model space would agree better with the empirical results.

The present GT results agree well with quenching observed in other nuclei, so it is likely that the method used here to normalize the measured cross section to GT strength could be successfully applied to other odd-even nuclei. We believe that in cases such as this one, in which the transition is of the ''jackknife'' type, the $0°$ charge exchange differential cross section is not proportional to the β-decay matrix element. We believe that to estimate the unit GT cross section, more reliable results are obtained using the known Fermi transition strength, its measured $0°$ cross section and the empirical relationship [1] between unit GT and unit F cross sections. This approach may solve the long standing discrepancy reported between even-even and odd-even targets used in (p,n) reactions to obtain unit GT cross sections. The present $\hat{\sigma}_{\mathrm{GT}}=10.5\pm0.5$ mb/sr indicates a smooth atomic number A dependence for this quantity, reported in Ref. [1]. These unit GT cross sections are used to empirically obtain GT strength distributions in nuclei which have important applications, such as neutrino detection [43].

ACKNOWLEDGMENTS

The authors would like to acknowledge the careful work done by Bill Lozowski in preparing the targets used in these runs, and also the crew of the IUCF Cyclotron. We also would like to thank J. J. Kelly for providing us the code ALLFIT. This paper was supported in part by the National Science Foundation.

[1] T. N. Taddeucci, C. A. Goulding, T. A. Carey, R. C. Byrd, C. D. Goodman, C. Gaarde, J. Larsen, D. Horen, J. Rapaport, and E. Sugarbaker, Nucl. Phys. **A469**, 125 (1987).
[2] C. Gaarde, J. S. Larsen, and J. Rapaport, in *Spin Excitations in Nuclei*, edited by F. Petrovich *et al.* (Plenum, New York, 1984), p. 65.
[3] F. Osterfeld, Rev. Mod. Phys. **64**, 491 (1992).
[4] T. Wakasa *et al.*, Phys. Rev. C **55**, 2909 (1997).
[5] T. N. Taddeucci, in *Anti-Nucleon and Nucleon-Nucleus Interactions*, edited by G. E. Walker, C. D. Goodman, and C. Olmer (Plenum, New York, 1985), p. 277.
[6] T. N. Taddeucci, in *Spin and Isospin in Nuclear Interactions*, edited by S. W. Wissink, C. D. Goodman, and G. E. Walker (Plenum, New York, 1991), p. 393.
[7] H. Sakai *et al.*, Nucl. Phys. **A599**, 197c (1996).
[8] C. D. Goodman *et al.*, Phys. Rev. Lett. **54**, 877 (1985).
[9] J. Rapaport *et al.*, Phys. Rev. C **36**, 500 (1987).
[10] M. Palarczyk *et al.*, Nucl. Instrum. Methods Phys. Res. A **457**, 309 (2001).
[11] V. Derenchuck *et al.*, *Proceedings from the 13th International Conference on Cyclotrons and Their Applications* (World Scientific, Vancouver, 1995).
[12] S. P. Wells *et al.*, Nucl. Instrum. Methods Phys. Res. A **235**, 205 (1992).
[13] T. N. Taddeucci *et al.*, Phys. Rev. C **41**, 2548 (1990).
[14] F. Ajzenberg-Selove, Nucl. Phys. **A523**, 1 (1991).
[15] J. J. Kelly, computer code ALLFIT (unpublished).
[16] J. J. Kelly, Ph. D. thesis, Massachusetts Institute of Technology, 1981.
[17] J. W. Watson *et al.*, Phys. Rev. Lett. **55**, 1369 (1985).
[18] W. -T. Chou, E. K. Warburton, and B. A. Brown, Phys. Rev. C **47**, 163 (1993).
[19] J. W. Watson and Q. Q. Du, in *New Facet of Spin Giant Resonances in Nuclei*, edited by H. Sakai, H. Okamura, and T. Wakasa (World Scientific, Singapore, 1998), p. 203.
[20] B. A. Brown *et al.*, the Oxford-Buenos Aires-MSU shell model code OXBASH, Michigan State University Cyclotron Report No. 524, 1986.
[21] E. K. Warburton and B. A. Brown, Phys. Rev. C **46**, 923 (1992).
[22] R. Schaeffer and J. Raynal, computer program DWBA70, 1970 (unpublished); extended version DW81 by J. R. Comfort, 1981 (unpublished).
[23] M. A. Franey and W. G. Love, Phys. Rev. C **31**, 488 (1985).
[24] W. G. Love (private communication).
[25] F. P. Brady *et al.*, Phys. Rev. C **43**, 2284 (1991).
[26] R. S. Hicks *et al.*, Phys. Rev. C **26**, 339 (1982).
[27] J. R. Comfort and B. C. Karp, Phys. Rev. C **21**, 2162 (1980).
[28] P. E. Hodgson, *Nuclear Reactions and Nuclear Structure* (Clarendon, Oxford, 1971).
[29] R. E. McDonald, J. A. Becker, R. A. Chalmers, and D. H. Wilkinson, Phys. Rev. C **10**, 333 (1974).
[30] J. L. Mildenberger *et al.*, Phys. Rev. C **43**, 1777 (1991).
[31] M. Ericson, A. Figureau, and C. Thevenet, Phys. Lett. **45B**, 19 (1973).
[32] E. Oset and M. Rho, Phys. Rev. Lett. **42**, 47 (1979).
[33] A. Bohr and B. Mottelson, Phys. Lett. **100B**, 10 (1981).
[34] K. Shimizu, M. Ichimura, and A. Arima, Nucl. Phys. **A226**, 282 (1974).
[35] G. F. Bertsch and I. Hamamoto, Phys. Rev. C **26**, 1323 (1982).
[36] I. S. Towner and F. C. Khanna, Nucl. Phys. **A399**, 334 (1983); I. S. Towner, Prog. Part. Nucl. Phys. **11**, 91 (1984).
[37] K. Ikeda, S. Fujii, and J. I. Fujita, Phys. Rev. Lett. **3**, 271 (1963).
[38] X. Yang *et al.*, Phys. Rev. C **52**, 2535 (1995).
[39] J. M. Moss, Phys. Rev. C **26**, 727 (1982).
[40] J. M. Moss, in *Spin Excitations in Nuclei*, edited by F. Petrovich, G. E. Brown, G. T. Garvey, C. D. Goodman, R. A. Lindgren, and W. G. Love (Plenum, New York, 1984), p. 355.
[41] D. J. Mercer *et al.*, Phys. Rev. C **49**, 3104 (1994).
[42] X. Y. Chen *et al.*, Phys. Rev. C **47**, 2159 (1993).
[43] J. N. Bahcall, in *Neutrino Astrophysics* (Cambridge University Press, Cambridge, 1989), p. 178.